ORGANOMETALLICS

Article

pubs.acs.org/Organometallics

Immobilization of Pyrene-Tagged Palladium and Ruthenium Complexes onto Reduced Graphene Oxide: An Efficient and Highly Recyclable Catalyst for Hydrodefluorination

Sara Sabater, José A. Mata,* and Eduardo Peris*

Departamento de Química Inorgánica y Orgánica, Universitat Jaume I, Avenida Sos Baynat s/n, 12071, Castellón, Spain

Supporting Information

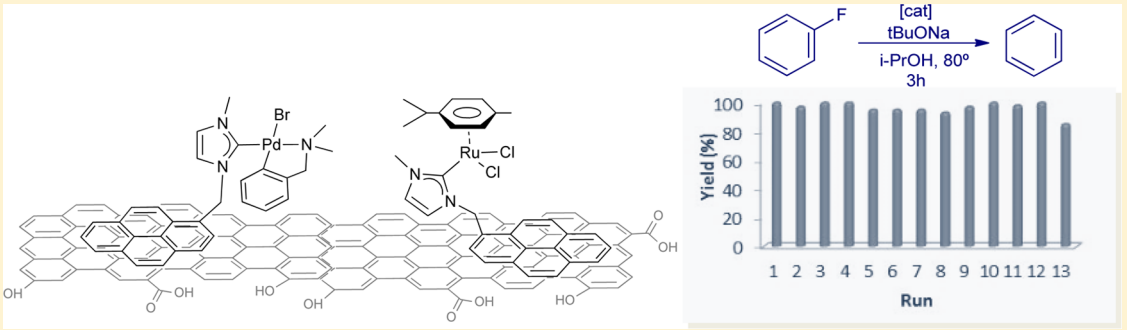

ABSTRACT: The co-immobilization of palladium and ruthenium complexes with pyrene-tagged N-heterocyclic carbene ligands onto reduced graphene oxide allows the formation of a highly efficient catalyst for the hydrodefluorination of a series of fluoroarenes. This procedure constitutes an easy one-pot preparation of materials with homogeneously distributed polymetallic catalysts. The catalytic system can be recycled up to 12 times without measurable loss of activity. The activity of the catalyst is attributed to the synergistic action of the two metals.

INTRODUCTION

The immobilization of a homogeneous catalyst onto a solid surface is one of the major challenges in catalysis, because it allows the separation of the catalyst and the reaction products, and may facilitate the reutilization of the catalyst in multiple subsequent cycles.[1] Carbon surfaces have recently gained attention as convenient supports for molecular attachment. Over the more widely used covalent immobilization strategies, which often require nontrivial pretreatment of the solid surface, noncovalent methods that use strong π interactions between polyaromatic hydrocarbons and graphitized surfaces have attracted great interest because they offer a convenient, nondestructive approach to catalyst immobilization.[1e] Due to the inherent capability of pyrene to afford noncovalent interactions with graphitic surfaces,[2] pyrene-containing metal complexes have been supported on graphitized surfaces[3] and have also been used in catalysis, proving interesting recyclability properties.[4] We recently obtained two complexes of palladium and ruthenium containing an N-heterocyclic carbene ligand with a pyrene tag, which were used for the hydrogenation of alkenes (palladium) and oxidation of alcohols (ruthenium).[5] We proved not only that the catalytic efficiencies of the catalysts were enhanced upon immobilization but also that the catalysts could be recycled 10 times without apparent loss of activity. Precisely, the combination of these two metals into a single-frame heterodimetallic complex allowed us to recently obtain a highly efficient catalyst for the hydrodefluorination of a wide set of fluoro-organic molecules.[6] Our studies showed that the overall process implies that the palladium fragment facilitates the C−F activation, while the ruthenium center allows the reduction of the substrate via transfer hydrogenation from *i*PrOH/*t*BuONa, in a clear example of synergistic behavior.

Hydrodefluorination (HDF) is the simplest C−F activation process, but it features a surprising mechanistic diversity.[7] The reaction formally implies the activation of a carbon−fluorine bond followed by the introduction of hydrogen to form the final hydrodefluorinated molecule. The reaction constitutes a great challenge in catalysis, because carbon−fluorine bonds lie among the most unreactive functionalities in chemistry.[8] Carbon−fluorine activation has been an active research field during the last three decades, but HDF has only flourished recently, probably triggered by the need for effective catalysts that allow the activation and disposal of the chlorofluorocarbons (CFCs), considered as "supergreenhouse gases".[9]

By combining our experience in the immobilization of pyrene-functionalized palladium and ruthenium complexes onto a reduced graphene oxide surface (rGO), with our experience in using mixed palladium/ruthenium complexes in catalytic HDF, we now report the immobilization of two complexes of palladium and ruthenium onto rGO and report a

Received: October 15, 2014

DOI: 10.1021/om501040x
Organometallics XXXX, XXX, XXX−XXX

Scheme 1

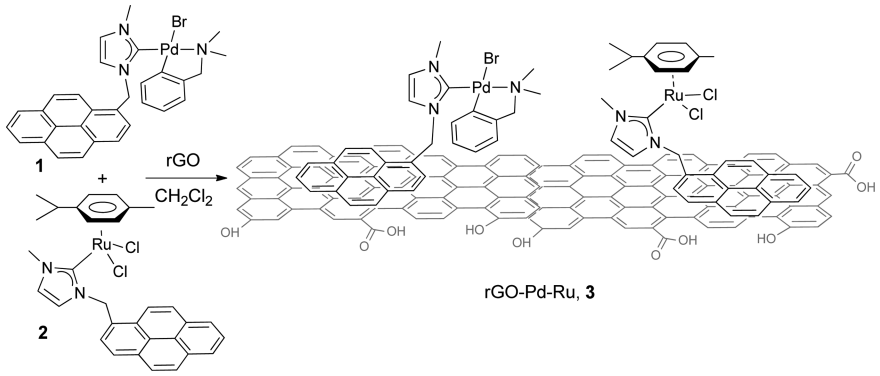

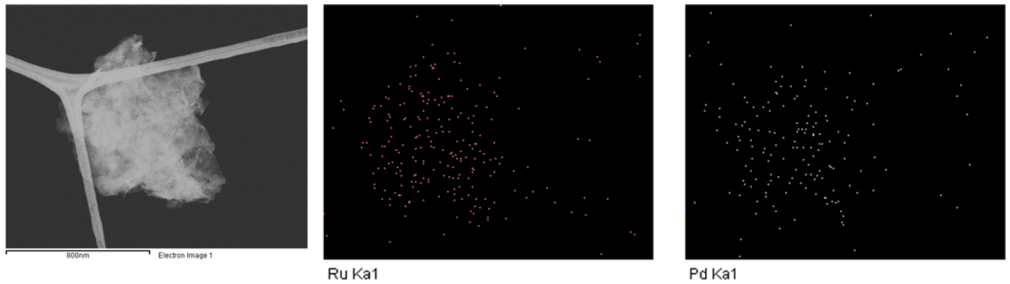

Figure 1. STEM image of rGO-Pd-Ru, **3** (left), and EDS elemental mapping images showing the homogeneous distribution of ruthenium (middle) and palladium (right).

study on the use of the resulting heterogenized catalyst in the HDF of a series of aromatic fluorocarbons.

RESULTS AND DISCUSSION

An equimolecular mixture of complexes **1** (Pd) and **2** (Ru) was supported onto reduced graphene oxide by mixing the molecular complexes and rGO in dichloromethane in an ultrasound bath for 30 min and stirring for 10 h (Scheme 1). The first indication that the immobilization has taken place is the loss of the color of the solution. The resulting rGO containing the two catalysts was filtered and washed with dichloromethane. The ^{1}H NMR spectrum of the filtrate revealed the absence of signals due to **1** or **2** and therefore constitutes indirect evidence that the two complexes have been effectively grafted on the solid surface. This methodology allows the simultaneous immobilization of different metal complexes onto the surface of rGO. The materials obtained show a homogeneous distribution of metals.

The exact palladium and ruthenium content in the final solid rGO-Pd-Ru, **3**, was determined by ICP-MS analysis after digestion of the solid in hot HCl/HNO_3. The results indicated a 5.19 and 4.97 wt % for palladium and ruthenium, respectively. The characterization of **3** was carried out by using UV/vis, FTIR, Ar-sorption experiments, AFM, and HRTEM (See Supporting Information for details). The UV/vis measurements (Figure S1) reveal that the spectrum of **3** consists of the overlap of the molecular complexes (**1** or **2**) with rGO, thus confirming the presence of the complexes on rGO, as seen by the characteristic pyrene UV/vis signals.[4b,10] For the determination of the surface area of the solid, the argon adsorption–desorption isotherms at 77 K were measured (most commonly referred to as BET surface area, where BET stands for Brunauer–Emmet–Teller). The BET area for **3** was 165 m^2 g^{-1}, significantly lower than that shown by the rGO raw material (373 m^2 g^{-1}). The elemental mapping by energy-dispersive X-ray spectroscopic analysis (EDS) performed by means of HRTEM of **3** confirmed the homogeneous distribution of palladium and ruthenium in the hybrid material (Figure 1).

In order to evaluate the activity of the palladium–ruthenium hybrid material **3** in HDF, we first tested its activity toward a series of fluoroarenes. The reactions were carried out in *i*PrOH at 80 °C, over 3 h and in the presence of *t*BuONa. The reactions were performed using 2 mol % of the catalyst, based on the amount of metal (in the case of the solid material **3**, the catalyst loading was 1 mol % of Ru and 1 mol % of Pd). For comparative purposes, we also tested the activity of rGO and the previously reported materials rGO-Pd and rGO-Ru, which contain only one of the two metal complexes grafted onto the solid surface.[5] We noticed that the supported catalysts needed to be activated prior to their use in the catalytic reactions. The activation of the catalysts was carried out by refluxing the solid in *i*PrOH in the presence of *t*BuONa, for 24 h. As can be seen from the results shown in Table 1, for the hydrodefluorination of fluorobenzene, it becomes clear that both rGO and rGO-Ru are completely ineffective, while the palladium-containing solid, rGO-Pd, produces moderate amounts (50%) of the defluorinated product (compare entries 1, 2, and 3). When complexes **1** and **2** are mixed together and used for the homogeneously catalyzed hydrodefluorination of fluorobenzene, we did not observe the formation of benzene. This result is rather surprising, especially if we compare it with the result obtained for the use of the heterogenized catalyst **3**, which afforded full conversion to benzene (compare entries 4 and 5). This "abnormal" enhancement in the activity of the immobilized catalyst onto the graphene material has already been observed before for catalysts supported on graphene oxide,[5,11] but this new example that we report here is far more striking because it

DOI: 10.1021/om501040x
Organometallics XXXX, XXX, XXX–XXX

Table 1. Hydrodefluorination of Fluoroarenes[a]

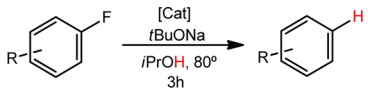

Entry	Catalyst	Substrate	Product	Yield (%) 1st run	Yield (%) 2nd run
1[b]	**rGO**			0	0
2[b,c]	**rGO-Ru**			0	0
3[c]	**rGO-Pd**			51	75
4[b]	**1**+**2**			3	--
5	**3**			100	100
6	**3**			52	60
7	**3**	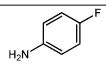	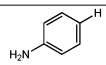	85	95
8	**3**	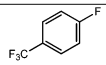	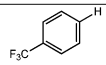	63	65
9[d,e]	**3**			50	50(90)
10[e,f]	**3**			43	45(63)

[a]Reactions were carried out with 0.3 mmol of fluoroarene, *t*BuONa (0.3 mmol), preactivated catalyst (1 mol % base on each metal), 2 mL of *i*PrOH for 3 h at 80 °C. Yields determined by GC analyses using anisole as internal standard. [b]GC yields after 20 h. [c]Catalyst loading 2 mol %. [d]Two equivalents of *t*BuONa (0.6 mmol). [e]Yields in parentheses are after 6 h. [f]Three equivalents of *t*BuONa (0.9 mmol).

shows that the catalyst is active only when it is immobilized onto the graphene surface. Catalyst **3** was also very active in the hydrodefluorination of 4-fluoroaniline and 4-fluorotrifluoromethyltoluene, and showed moderate activity for the C−F activation of 4-fluorotoluene, 1,4-difluorobenzene, and 1,3,5-trifluorobenzene, although the conversions increased upon increasing the reaction times (see entries 9 and 10).

In order to test if the activity of the catalysts could be maintained upon catalyst recovery, we performed a second run by recycling the catalyst from the reaction mixture. As can be seen from the results shown, the activity of the palladium-supported catalyst, rGO-Pd, improved with respect to the first cycle (entry 3, first run 50%, second run 75%). This result is probably due to the activation of the catalyst along the reaction course and may be ascribed to the slow formation of palladium nanoparticles. In the case of the heterometallic solid material, **3**, we also observed that the activity was maintained for the case of the hydrodefluorination of fluorobenzene (entry 5). For the hydrodefluorination of the rest of the substrates that we tested, we observed a slight enhancement of the catalytic activity, again probably as a consequence of the formation of active palladium nanoparticles (see below for further analysis and discussion). As can be seen from the results shown in the table, despite the fact that the palladium-containing material, rGO-Pd, is active in the hydrodefluorination of fluorobenzene, its activity is much lower than that shown by the Ru−Pd material, **3**, which affords better results even using a lower loading of palladium (rGO-Pd contains 2 mol % of palladium, while **3** contains 1 mol % of palladium). This result verifies our initial hypothesis that the synergistic role of the two metals is playing an important role in the catalytic performance of our hybrid catalyst **3**. The high-resolution images of transmission electron microscopy (HRTEM) of **3** after being activated showed the formation of well-dispersed small nanoparticles (<5 nm diameter). The analysis by energy-dispersive X-ray spectroscopy (EDS) performed by means of HRTEM of **3** did not provide any definitive information about whether these nanoparticles were formed by Pd, Ru, or a mixture of these two metals (see Figure S9 in the SI for details). In order to determine the nature of these nanoparticles, we performed a control experiment by independently incubating the palladium- and ruthenium-supported catalysts (rGO-Pd and rGO-Ru) in *i*PrOH at 80 °C in the presence of *t*BuONa during 24 h. The HTREM images of the incubated samples showed that only the rGO-Pd material developed nanoparticles (Figure S12 in the SI). The palladium content of the nanoparticles was further confirmed by the EDS spectrum of the sample (Figure S13 in the SI). For the rGO-Ru sample, the energy-dispersive X-ray spectroscopic analysis performed by means of scanning transmission electron microscopy (STEM) confirmed the homogeneous distribution of ruthenium in the solid (Figure S11 in SI), and this time we did not detect the presence of nanoparticles. This result indicates that the small nanoparticles formed when **3** is used are formed by palladium, which has a higher tendency to aggregate than ruthenium under the reaction conditions used, as we previously demonstrated.[5] This finding should explain the differences found in the catalytic activity of the solid material **3**, compared to the inactive catalytic system formed by the mixture of the two homogeneous catalysts **1** and **2**. Also, the mechanism for this process is different from the mechanism for our previously described homogeneous Ru−Pd catalyst.[6] In this case, we believe that the C−F activation should be promoted by the palladium nanoparticles, while the introduction of the hydrogen by transfer hydrogenation should be facilitated by the ruthenium heterogenized complex, and therefore the synergistic action between the two metals is crucial for explaining the superior activity of the catalyst.

We were interested in determining if we could recycle catalyst **3** for several catalytic cycles without loss of its catalytic activity. The recycling experiments were performed using fluorobenzene as model substrate. The reaction conditions used were the same as those shown in Table 1, and the reaction progress was determined by GC. After completion of each run (3 h), the reaction mixture was allowed to reach room temperature, and the solid catalyst was separated by centrifugation, washed with CH_2Cl_2, dried, and reused in the subsequent cycle. Each cycle required the addition of one equivalent of *t*BuONa with respect to fluorobenzene. By following this procedure, catalyst **3** could be recycled for up to 12 runs, without any observable decrease of activity. Only during the 13th run did we observe a decrease in activity to 85%, but we believe that this result may be due to the accumulated loss of catalyst during the successive filtrations. The ICP-MS analysis after the first run accounted for 4.87 wt % of ruthenium and 4.99 wt % of palladium, indicating a negligible loss of metals. When the ICP-MS analysis was carried out after the final 13 runs, we did observe that the total amount of metals found was 3.94 wt % for ruthenium and 3.85 wt % for palladium, indicating an approximate 20% loss of metal with respect to the initial content. However, this loss of percent of metal content may be due to the mass gain during the

DOI: 10.1021/om501040x
Organometallics XXXX, XXX, XXX−XXX

subsequent cycles due to the adsorption of substances from the catalyst reactions (we believe that a mass gain due to *t*BuONa adsorption may have occurred, as we previously observed),[5] so it may not be ascribed to desorption or leaching of the metal complex. The atomic force microscopy measurements (AFM) of **3** before and after its activation revealed that the height of the rGO sheets is about 2 and 1.5 nm, respectively, both within the accepted range of few-layer graphenes.[12] Interestingly, the BET surface area of **3** is 164 and 221 m^2/g for the unactivated and activated materials, respectively. These data are in agreement with the data coming from the AFM analysis, which suggests a partial exfoliation of the catalyst upon activation.

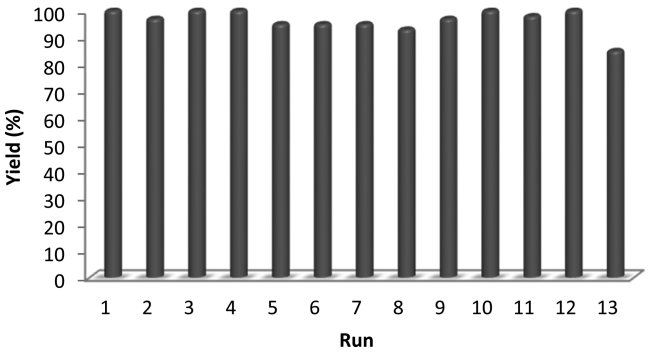

Figure 2. Recycling experiments of hydrodefluorination of fluorobenzene in the presence of **3**. The reactions were carried out in *i*PrOH in the presence of *t*BuONa, at 80 °C. After each run (3 h), the catalyst was filtered, washed with CH_2Cl_2, and dried. Run number 13 was carried out under air and using technical grade *i*PrOH.

We also performed an analysis of the reaction profiles of the hydrodefluorination of fluorobenzene using catalyst **3**. The time-course reaction profiles are shown in Figure 3 and are displayed for eight successive cycles. The reactions were monitored by ^{19}F NMR spectroscopy. We were interested in observing the activation process of the catalyst, and thus we started the experiments using the unactivated version of **3**. As can be seen from the profiles shown in Figure 3, the curve

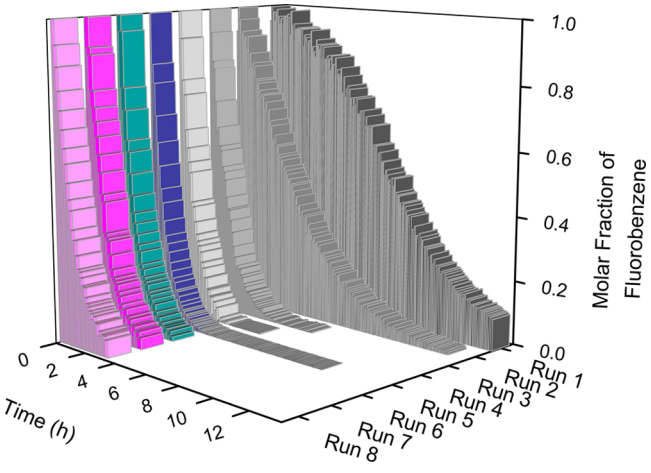

Figure 3. Reaction profiles for eight successive cycles of the hydrodefluorination of fluorobenzene with **3**. The reactions were carried out in *i*PrOH in the presence of *t*BuONa, at 80 °C. After each run, the catalyst was filtered, washed with CH_2Cl_2, and dried. The monitoring of the reactions was carried out by ^{19}F NMR spectroscopy.

corresponding to the first run has a sigmoidal form, indicating that the rate of formation of benzene is slowly increased with the reaction time, as a consequence of the gradual activation of the catalyst. Run 2 needs 12 h to complete, and runs 3 to 8 display quasi-identical profiles, achieving completion in about 3 h. The similarities of the reaction profiles displayed for runs 3–8 are a very good indication that the catalyst deactivation is negligible.

CONCLUSIONS

In summary, we have obtained a very effective catalyst for the hydrodefluorination of aromatic fluoroarenes. The catalyst is formed by a mixture of palladium and ruthenium complexes with a pyrene-NHC ligand, which are grafted on the surface of reduced-graphene oxide, by π-stacking interactions. The analysis of the catalyst before and after being used in the catalytic reaction indicates that small nanoparticles presumably formed by palladium aggregates, which together with the ruthenium-heterogenized complex may form the active catalytic system. The catalyst can be recycled up to 12 runs, without any decrease of activity and affording the quantitative hydrodefluorination of fluorobenzene. The reaction profiles of the process clearly show that the rate of hydrodefluorination slowly increases with the reaction time during the first run, in a clear indication that the catalyst needs an incubation time for its full activation. As inferred by the analysis of the solids after being used in the catalytic reaction, the activation consists of the formation of palladium nanoparticles; thus the catalytic hybrid system consists of a combination of palladium nanoparticles and the ruthenium molecular compound. The resulting catalyst can be recycled up to 12 times in the hydrodefluorination of fluorobenzene, with minimum loss of activity, thus showing great potential practical applications. We strongly believe that the simplicity of the design of this heterogeneous catalytic system, in combination with its great catalytic performance and recyclability, may inspire future research in the field of hydrodefluorination.

EXPERIMENTAL SECTION

General Procedures. All manipulations were carried out under nitrogen using standard Schlenk techniques and high vacuum, unless otherwise stated. Anhydrous solvents were obtained using a solvent purification system (SPS MBraun) or purchased from commercial suppliers and degassed prior to use by purging with dry nitrogen and kept over molecular sieves. Complexes **1** and **2** were obtained according to published methods.[5] Graphitic oxide (GO) was prepared from graphite powder (natural, universal grade, 200 mesh, 99.9995%) by the Hummers method,[13] and reduced graphene oxide was prepared by reduction of a colloidal suspension of exfoliated GO sheets in water with hydrazine hydrate.[14] All other reagents were used as received from commercial suppliers. NMR spectra were recorded on Varian Innova spectrometers operating at 300 or 500 MHz (^1H NMR) and 75 and 125 MHz (^{13}C NMR), respectively. Elemental analyses were carried out in an EA 1108 CHNS-O Carlo Erba analyzer. Infrared spectra (FTIR) were recorded on a JASCO FTIR-6200 spectrometer with a spectral window of 4000–500 cm^{-1}. Atomic force microscopy measurements were carried out with a JSPM-5200 JEOL scanning probe microscope using contact mode. High-resolution transmission electron microscopy images and high-angle annular dark-field (HAADF)-STEM images of the samples were obtained using a Jem-2100 LaB6 (JEOL) transmission electron microscope coupled with an INCA Energy TEM 200 (Oxford) energy dispersive X-ray spectrometer operating at 200 kV. The UV/vis spectra were recorded between 200 and 600 nm by a Cary 300 Bio UV/vis Varian spectrophotometer. The determination of the metal content in the

DOI: 10.1021/om501040x
Organometallics XXXX, XXX, XXX–XXX

solids was done by an ICP-MS Agilent 7500 CX. The digestion of the samples was carried out under reflux of a mixture of concentrated nitric and hydrochloric acids (3:1) for 12 h. The digestion of the samples after the recycling experiments was carried out after several washes with milli-Q water (10 × 10 mL).

Preparation of rGO-Pd-Ru, 3. In a round-bottom flask were introduced 270 mg of rGO, 30 mg of an equimolecular mixture of metal complexes **1** (15.2 mg, 0.025 mmol) and **2** (14.8 mg, 0.025 mmol), and 10 mL of CH_2Cl_2. The suspension was sonicated for 30 min and stirred at room temperature for 10 h until the solution become clear. The black solid was filtrated and washed with 2 × 15 mL of CH_2Cl_2, affording the resulting product as a black solid. The filtrates were combined and evaporated to dryness under reduced pressure. The amount of unsupported complexes **1** and **2** was analyzed by ^{1}H NMR using anisole as internal standard. Integration of the characteristic signal of anisole (−O*Me*) vs (NCH_2-Pyr) reveals the amount of complex that has been deposited on the rGO. The exact amount of complex supported was determined by ICP-MS analysis. Digestion of the material was performed in hot HCl/HNO_3. The palladium content is 5.19 wt %, and the ruthenium content 4.97 wt %.

General Procedure for the Catalytic HDF. In a typical experiment the catalyst (1 mol % based on each metal) and *t*BuONa (0.3 mmol) were placed together in a thick-walled Schlenk tube with a Teflon cap. The tube was then evacuated and filled with nitrogen three times. 2-Propanol (2 mL) was added, and the mixture was stirred at 80 °C for 24 h. Then fluoroarene (0.3 mmol) and anisole (0.3 mmol) were added, and the mixture was stirred at 80 °C for 3 h. Yields were determined by GC analyses using anisole as internal standard.

The recycling experiments were carried out under identical reaction conditions as described in the HDF procedure. After completion of each run, the reaction mixture was allowed to reach room temperature and centrifuged. The remaining solid was washed thoroughly with CH_2Cl_2 (5 × 10 mL), dried, and reused in the following run.

^{19}F NMR Monitoring Experiments. A J. Young's NMR tube was loaded with catalyst (1 mol % based on each metal) and *t*BuONa (0.3 mmol). The tube was then evacuated and filled with nitrogen three times. 2-Propanol (2 mL) and fluoroarene (0.3 mmol) were added. The tube was then introduced in an NMR probe preheated at 80 °C. The conversion of fluorobenzene was monitored by ^{19}F NMR spectroscopy at intervals over the course of the desired time. After completion of each run, the reaction mixture was allowed to reach room temperature and centrifuged. The remaining solid was washed thoroughly with CH_2Cl_2 (5 × 10 mL), dried, and reused in the following run.

■ ASSOCIATED CONTENT

Supporting Information

Full characterization of hybrid materials including UV/vis and FTIR spectroscopy, HRTEM, and AFM images. This material is available free of charge via the Internet at http://pubs.acs.org.

■ AUTHOR INFORMATION

Corresponding Authors

*E-mail: jmata@uji.es. Fax: (+34) 964387522. Tel: (+34) 964387516.

*E-mail: eperis@uji.es.

Notes

The authors declare no competing financial interest.

■ ACKNOWLEDGMENTS

We thank the financial support from the Ministerio de Ciencia e Innovación of Spain (CTQ2011-24055/BQU). We would also like to thank the "Generalitat Valenciana" for a fellowship (S.S.). The authors are grateful to the "Serveis Centrals d'Instrumentació Científica (SCIC)" of the Universitat Jaume I for providing spectroscopic X-ray facilities.

■ REFERENCES

(1) (a) Jones, C. W. *Top. Catal.* **2010**, *53*, 942−952. (b) Wang, Z.; Chen, G.; Ding, K. L. *Chem. Rev.* **2009**, *109*, 322−359. (c) Gladysz, J. A. *Chem. Rev.* **2002**, *102*, 3215−3216. (d) Coperet, C.; Chabanas, M.; Saint-Arroman, R. P.; Basset, J. M. *Angew. Chem., Int. Ed.* **2003**, *42*, 156−181. (e) Fraile, J. M.; Garcia, J. I.; Mayoral, J. A. *Chem. Rev.* **2009**, *109*, 360−417. (f) Bond, G. C. *Chem. Soc. Rev.* **1991**, *20*, 441−475.

(2) (a) Georgakilas, V.; Otyepka, M.; Bourlinos, A. B.; Chandra, V.; Kim, N.; Kemp, K. C.; Hobza, P.; Zboril, R.; Kim, K. S. *Chem. Rev.* **2012**, *112*, 6156−6214. (b) Rodriguez-Perez, L.; Herranz, M. A.; Martin, N. *Chem. Commun.* **2013**, *49*, 3721−3735.

(3) (a) Le Goff, A.; Reuillard, B.; Cosnier, S. *Langmuir* **2013**, *29*, 8736−8742. (b) Mann, J. A.; Rodriguez-Lopez, J.; Abruna, H. D.; Dichtel, W. R. *J. Am. Chem. Soc.* **2011**, *133*, 17614−17617.

(4) (a) Keller, M.; Colliere, V.; Reiser, O.; Caminade, A.-M.; Majoral, J.-P.; Ouali, A. *Angew. Chem., Int. Ed.* **2013**, *52*, 3626−3629. (b) Wittmann, S.; Schaetz, A.; Grass, R. N.; Stark, W. J.; Reiser, O. *Angew. Chem., Int. Ed.* **2010**, *49*, 1867−1870. (c) Kang, P.; Zhang, S. H.; Meyer, T. J.; Brookhart, M. *Angew. Chem., Int. Ed.* **2014**, DOI: 10.1002/anie.201310722.

(5) Sabater, S.; Mata, J. A.; Peris, E. *ACS Catal.* **2014**, *4*, 2038−2047.

(6) Sabater, S.; Mata, J. A.; Peris, E. *Nat. Commun.* **2013**, *4*, 2553−2559.

(7) (a) Amii, H.; Uneyama, K. *Chem. Rev.* **2009**, *109*, 2119−2183. (b) Kuehnel, M. F.; Lentz, D.; Braun, T. *Angew. Chem., Int. Ed.* **2013**, *52*, 3328−3348. (c) Meier, G.; Braun, T. *Angew. Chem., Int. Ed.* **2009**, *48*, 1546−1548. (d) Nova, A.; Mas-Balleste, R.; Lledos, A. *Organometallics* **2012**, *31*, 1245−1256. (e) Whittlesey, M. K.; Peris, E. *ACS Catal.* **2014**, *4*, 3152−3159. (f) Chen, Z.; He, C.-Y.; Yin, Z.; Chen, L.; He, Y.; Zhang, X. *Angew. Chem., Int. Ed.* **2013**, *52*, 5813−5817. (g) Baumgartner, R.; McNeill, K. *Environ. Sci. Technol.* **2012**, *46*, 10199−10205.

(8) (a) Douvris, C.; Ozerov, O. V. *Science* **2008**, *321*, 1188−1190. (b) Ahrens, M.; Scholz, G.; Braun, T.; Kemnitz, E. *Angew. Chem., Int. Ed.* **2013**, *52*, 5328−5332.

(9) (a) Han, W.; Li, Y.; Tang, H.; Liu, H. *J. Fluorine Chem.* **2012**, *140*, 7−16. (b) Shine, K. P.; Sturges, W. T. *Science* **2007**, *315*, 1804−1805. (c) Molina, M. J.; Rowland, F. S. *Nature* **1974**, *249*, 810−812. (d) Rowland, F. S.; Molina, M. J. *Rev. Geophys.* **1975**, *13*, 1−35. (e) Rowland, F. S.; Molina, M. J.; Chou, C. C. *Nature* **1975**, *258*, 775−776.

(10) (a) Ehli, C.; Guldi, D. M.; Herranz, M. A.; Martin, N.; Campidelli, S.; Prato, M. *J. Mater. Chem.* **2008**, *18*, 1498−1503. (b) Herranz, M. A.; Ehli, C.; Campidelli, S.; Gutierrez, M.; Hug, G. L.; Ohkubo, K.; Fukuzumi, S.; Prato, M.; Martin, N.; Guldi, D. M. *J. Am. Chem. Soc.* **2008**, *130*, 66−73. (c) Kavakka, J. S.; Heikkinen, S.; Kilpelainen, I.; Mattila, M.; Lipsanen, H.; Helaja, J. *Chem. Commun.* **2007**, 519−521.

(11) Zhao, Q.; Chen, D.; Li, Y.; Zhang, G.; Zhang, F.; Fan, X. *Nanoscale* **2013**, *5*, 882−885.

(12) Geim, A. K.; Novoselov, K. S. *Nat. Mater.* **2007**, *6*, 183−191.

(13) Hummers, W. S.; Offeman, R. E. *J. Am. Chem. Soc.* **1958**, *80*, 1339−1339.

(14) Stankovich, S.; Dikin, D. A.; Piner, R. D.; Kohlhaas, K. A.; Kleinhammes, A.; Jia, Y.; Wu, Y.; Nguyen, S. T.; Ruoff, R. S. *Carbon* **2007**, *45*, 1558−1565.

DOI: 10.1021/om501040x
Organometallics XXXX, XXX, XXX−XXX